ISSN 1392 - 1207. MECHANIKA. 2008. Nr.4(72)

Cracking behavior of electrodeposited nanocrystalline tungsten-cobalt and tungsten-iron coatings

V. Vasauskas*, J. Padgurskas*, R. Rukuiža*, H. Cesiulis, J.-P. Celis***, D. Milčius****, I. Prosyčevas*****

*Lithuanian University of Agriculture, Studentų 15, Akademija, 53361 Kauno r., Lithuania, E-mail: juozas.padgurskas@lzuu.lt, raimundas.rukuiza@lzuu.lt

**Vilnius University, Naugarduko 24, 03225 Vilnius, Lithuania, E-mail: henrikas.cesiulis@chf.vu.lt

***Katholieke Universiteit Leuven, Kasteelpark Arenberg 44, B-3001 Leuven, Belgium, E-mail: jean-pierre.celis@mtm.kuleuven.be

****Lithuanian Energy Institute, Breslaujos 3, 44403 Kaunas, Lithuania, E-mail: milcius@mail.lei.lt

*****Kaunas University of Technology, Savanorių 271, 50131 Kaunas, Lithuania, E-mail: igorpros@mail.ru

1. Introduction

The use of micrometer thick coatings in tribosystems is of increasing interest in the area of mechanical engineering in order to reduce friction and wear [1, 2]. Among common surface engineering processes, electroplating is one of the best available technologies. It finds increasing applications in electronics and microsystems because of its low price, relatively simple technological equipment, low energy consumption, achievable high precision, and mass production. It is attractive from an environmental point of view because the material deposition or removal achieved is highly selective thus minimizing losses; it can be operated as a "close box" process, and has already been made compatible with "clean room" practice in microelectronics [3, 4]. Electrochemical deposition is the most convenient to get alloys with high melting points, such as tungsten or molybdenum alloys.

Electrodeposited tungsten alloys containing iron group metals are attractive from various points of view inclusive tribology. The presence of tungsten in amorphous alloys increases the corrosion resistance of such alloys [5-9]. Additionally, tungsten alloys are of growing interest for their unique combination of tribological, magnetic, electrical, electro-erosion properties and attractive mechanical properties (e.g. high tensile strength and premium hardness), good resistance to strong oxidizing acids, and high melting temperature [10-12]. Usually, electrodeposited coatings of tungsten alloys are nano-crystalline and hard. Therefore they might be attractive for various applications in microelectronics and micromechanics.

The yield strength as a measure for the onset of plastic deformation is a very important property of wear and/or corrosion protective coatings [13]. Since the mechanical properties of coatings can significantly differ from those of corresponding bulk materials, they have to be determined independently. The determination of yield strength of hard and brittle coatings is very difficult and cannot be done by conventional methods like tensile tests. However, the experimental difficulties increase when the yield strength of thin hard coatings deposited on soft substrates has to be determined, because the yield strength of the substrate will be exceeded before plastic deformation in the film is reached. Hard and stiff protective coatings offer an effective resistance to sliding. However, such coatings also tend to be brittle, and therefore are susceptible to failure under high loads, especially in sharp contacts ($2\Theta < <120^{o}$) [14].

The characterization procedure for coatings must be relatively simple, nondestructive, and cost-effective. Indentation test modeling of, e.g. hardness tests, resulted in a simple composite hardness relation and failure morphology based on area functions, and in the analysis of film and substrate [15]. The crack formation in coatings is schematically drawn in Fig. 1. Radial plastic deformation zone results in a circumferential cracking of the film outside the contact area of the indenter.

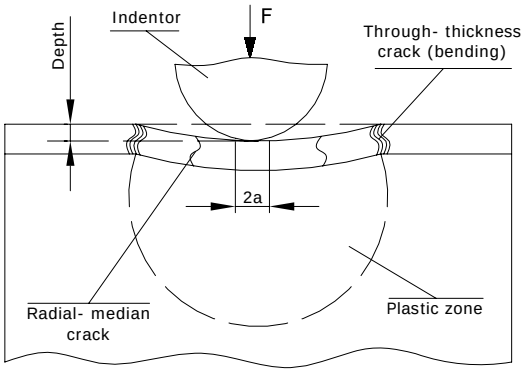

Fig. 1 Formation of through-thickness cracks under indentation. Cracks are positioned at the boundary of plastic zone in the substrate

Two variations were proposed, either film bending under strain to match the indenter shape, or cracking within the indentation zone. On hard substrates, coatings bend to match the indenter shape, whilst cracking of the coating can arise on soft substrates. Both sharp and blunt indenters can be used to produce cracks in brittle solids. Sharps indenters, such as a Vickers diamond pyramid indenter, produce subsurface radial cracks along tensile median planes, whereas blunt indenters, such as hard spherical or cylindrical indenters, produce the well-known Hertzian cone crack [16].

This work was initiated to analyze critically the deformation of electrodeposited Co-W and Fe-W coatings resulting from indentation tests, and to identify the microscopic features of the surfaces of such electrodeposited layers.

2. Experimental

Alloyed tungsten coatings were electrodeposited on mechanically polished copper and steel (ST3) substrates. Just before electrodeposition, the substrates were degreased and activated in 5% sulfuric acid, then a nickel seed-layer was electroplated for 1 min. from a Wood's nickel electrolyte containing 240 g/l $NiCl_2$ $6H_2O$ + 80 g/l HCl at 30 mA/cm^2. Then, alloy coatings were electrodeposited from citrate-ammonia baths containing 0.2M $CoSO_4$ (or $FeSO_4$) + 0.5M Na_2Hcitr + 0.4M Na_2WO_4 at 30 mA cm^{-2}. The thickness of the coatings was about 10 to 15 μm as determined by gravimetry. The investigated Co-W and Fe-W alloys have the composition 72 at. % Co + + 28 at. % W, and 69 at. % Fe + 31 at. % W respectively.

The buffer capacity of the plating bath solution was determined by titration with 15 M NaOH solution to avoid any dilution effects. Changes in pH were monitored by a pH-meter (ThermoOrion, type 420). Buffer capacity values at certain pH were extracted after numerical differentiation of titration curves.

X-ray diffraction (XRD) analyses were performed in order to determine grain size and texture of the electrodeposited films. A Dron instrument (type 3.0) with Ni filtered Cu–$K_{\alpha 1}$ radiation (30 kV and 30 mA, λ=1.54056 Å) was used at a continuous scan speed of 0.02° 2θ s^{-1}.

Vickers microhardness and adhesion were determined by VDI Rockwell indentation at 2 kN load for coatings of different thickness. A microhardness tester (PMT-3) operated with a Vickers indenter was also used to determine the indentation characteristics of the coatings. It was assumed that the quasiplastic zone contains incipient cracks of the same length scale as the quasiplastic zone dimension [15]. Taking into account that the value of h (F) depends on the respective hardness (H), the following equation is valid for sharp indenters [15]

$$H = \frac{F}{cd^2} \tag{1}$$

$$\text{or} \quad d = \sqrt{\frac{F}{cH}} \tag{2}$$

where F is the applied load, d is the length of the diagonal of the indent, and c is constant. Eq. (1) is based on the assumption of a size invariant hardness.

Diagonal length of the indentation was determined from both optical (OM) and scanning microscopy (SEM). In VDI Rockwell indentation tests only plastic deformation distribution around indentations was observed. The loads necessary to induce extensive delamination and fracture of the coatings were derived based on these experiments.

3. Result and discussions

3.1. CoW and FeW electrodeposited coatings and initial features of these deposits

The electrodeposition was done in citrate-ammonia baths. A distinctive feature of such baths is the strong effect of their pH on current efficiency and composition of the electrodeposited alloys [17]. Moreover, during the electrodeposition of W-alloys, the electro reduction of WO_4^{2-}-ions to W is associated with an increase of the pH in the double layer

$$WO_4^{2-} + 4H_2O + 6e = W + 8OH^- \tag{3}$$

In addition, the electrodeposition of W-alloys is accompanied by H_2 evolution

$$2H_2O + 2e = H_2 + 2OH^- \tag{4}$$

That yields an alkalization of the electrochemical double layer, what in general [7, 9, 17-19] decreases the W-content in the electrodeposited coatings.

Therefore, in order to achieve electrodeposited coatings with high tungsten content, plating baths with a high buffer capacity are required. From Fig. 2 it appears that the buffer capacity at room temperature at pH between 6.5 and 9 is not strongly affected by the amount of ammonia but is mainly controlled by the presence of citrates. A maximal buffer capacity is obtained at pH 7.25. After addition of ammonia to the solution, two maxima and a deep minimum are noticed at pH ~8.5. The maximum buffer capacity noticed at pH 10-10.5 apparently depends on the concentration of ammonia.

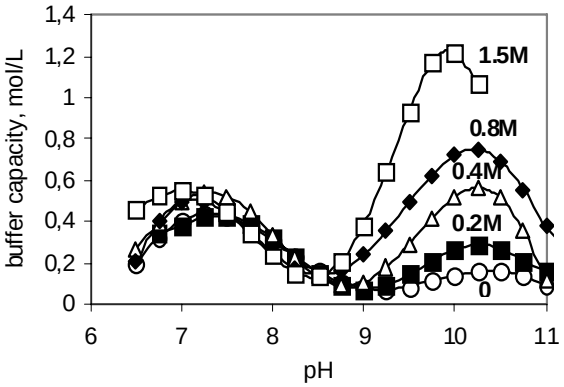

Fig. 2 Buffer capacity vs. pH for various ammonia concentrations (23°C). The concentration of ammonia in solution is indicated next to the curves. Formulation of the solution: 0.2M $CoSO_4$ + 0.5M Na_2HCitr + + 0.4M Na_2WO_4

Since electrodeposition of W alloys is usually carried out at elevated temperatures, the buffering properties of solutions at elevated temperatures are also of importance. The comparison of the buffer capacity of solutions at high ammonia concentrations for different temperatures is given in Fig. 3. When the concentration of ammonia is 0.8 M, the minimum in buffer capacity is at 70°C being not as deep as at room temperature. When the concentration of ammonia increases, the minimum in buffer capacity even disappears.

The electrodeposition from aqueous baths is usually carried out in nonhermetic cells. In such cases, a part of ammonia can evaporate during long-term electrodeposition at elevated temperatures. That results in the decrease of deposition rate. Therefore, the electro-deposition was performed at pH as low as possible. The main experiments were done at pH 7.5-8.1. Under such plating conditions, a sufficient part of ammonia added to the solutions trans-

forms into nonvolatile NH_4^+-ionic compounds. Moreover, because of the better buffering capacity of solutions at these pH, a higher concentration of ammonia (e.g.1.5 M) is used.

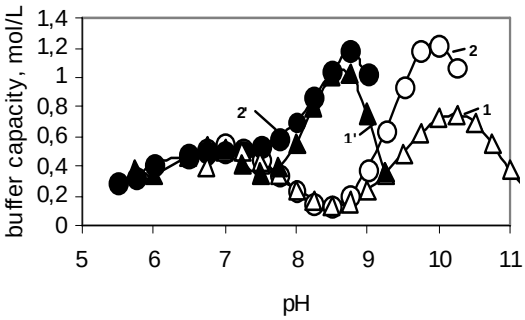

Fig. 3 Buffer capacity vs. pH at different temperatures. Formulation of the solution: 0.2M $CoSO_4$ + 0.5M Na_2HCitr + 0.4M Na_2WO_4 + xM ammonia. 1 and 1' for x=0.8M; 2 and 2' for x=1.5M. 1 and 2 at 23°C; 1' and 2' at 70°C

The values of buffer capacity are similar in the presence either Co(II) or Fe(II) salts because of their similar complexation by citrates, ammonia and hydroxide ligands [20]. In view of that, a solution containing: 0.2M $MeSO_4$ + 0.4M Na_2WO_4 + 0.5M Citric acid + 1.5M ammonia water was selected. The pH was adjusted by adding H_2SO_4 or NaOH. "Me" means the iron group metal (Co or Fe). Electrodeposition was carried out at 70°C. The highest W-content was obtained at pH ranging from 7.0 to 8.1. The W-content can even exceed 30 at. %, whereas alloys with a lower W-content (max. ~22 at. % of W) are obtained at lower or higher pH. Because of the high concentration of Co(II) or Fe(II), and W(VI) in the bath, the current efficiency can exceed 40% in the case of Co-W electrodepositing, and 30% in the case of Fe-W electrodeposition.

From the X-ray diffractograms of elctrodeposited Co-W and Fe-W alloys shown in Fig. 4, it seems that the addition of tungsten to the alloys modifies the crystallographic texture. The introduction of tungsten into alloys results the transformation of the texture: it transforms from the polycrystalline which is regular for pure electrodeposited Co and Fe, into deformed (111) texture for CoW, and (110) – for FeW alloys. Deformation of the structure causes the slight shifting of the peak position in the XRD spectra. Such shift is characteristic for tungsten alloys [5, 7]. A widening of the single diffraction peaks appears when the amount of tungsten exceeds 20 at. % indicating that the grain size of the electrodeposited W-containing alloys (both Co-W and Fe-W) decreases. The mean crystallite size was calculated from the peak width using Scherrer's equation for pure Co and Fe, and the modified Scherrer's equation by Warren and Biscoe

$$\beta = \frac{0.94\lambda}{\tau \cos\Theta} \tag{5}$$

$$\beta = B^2 - b^2 \tag{6}$$

where β is the peak broadening (in radians); λ is the wavelength (in Å); τ is the grain size; Θ is the position of the peak in diffractogram; b is the width of the peak for the crystalline material; and B is the peak width of the sample examined.

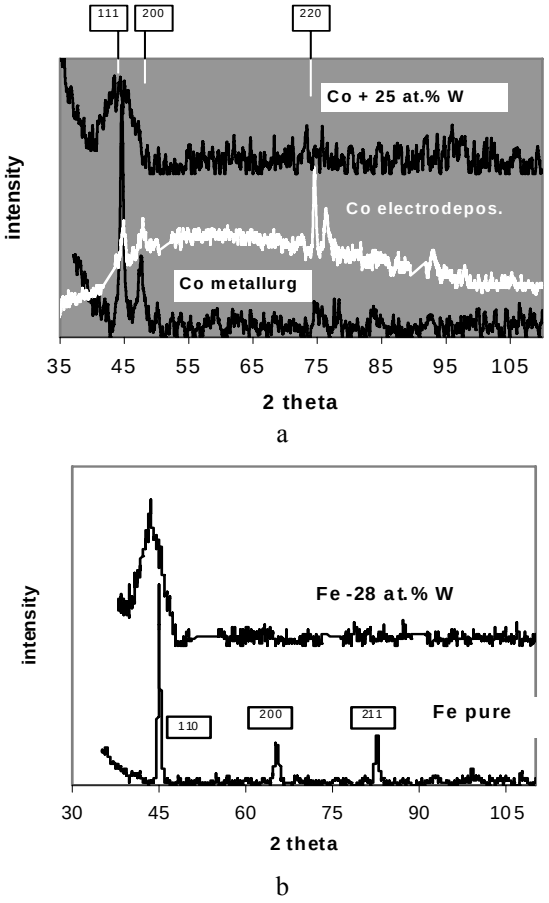

Fig. 4 XRD patterns for Co, Fe and their alloys: a - metallurgical pure Co, electrodeposited pure Co, and electrodeposited Co+25 at. % W; b - metallurgical Fe and electrodeposited Fe-31 at. % W. The XRD lines are marked next to the corresponding pattern

In our case, the value of b was experimentally determined for Co (111) or Fe (110) peak of polycrystalline pure metals as described in [9]. From the data given in Table, the grain size of electrodeposited Co-W and Fe-W alloys is approx. 3 - 4 nm that allows to concern the structure as nanocrystalline. Electrodeposits with such a small grain size may be of interest for various applications comprising micromechanics as well.

Table
XRD data of electrodeposited W-containing alloys and calculated crystallite sizes

Metal or alloy	2Θ position of (111) peak, deg	Peak broadening, rad	Estimated grain size, nm
Co (electrodeposited)	44.85	0.00375	41.7
Co-W (25 at. % of W) (electrodeposited)	43.98	0.0525	3.0
Fe (metallurgical)	44.85	0.00375	41.7
Fe-W (28 at. % of W) (electrodeposited)	43.40	0.0424	3.7

Electrodeposited Co-W and Fe-W alloys look

white, bright and smooth (see Fig. 5 and 6). Based on the 3D surface analysis the mean roughness (R_a) was in the range 200 to 500 nm.

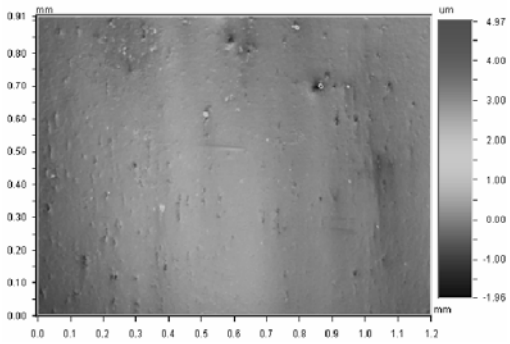

Fig. 5 3D image used for Co-W (25 at. % of W) roughness estimation

The electrodeposited alloys exhibit high hardness (Fig. 7). The hardness determined by nano-indentation close to the surface is approx. 20 to 30% higher than in the bulk. Probably, this might be associated with oxide formation on top of the coating, since oxides are expected from

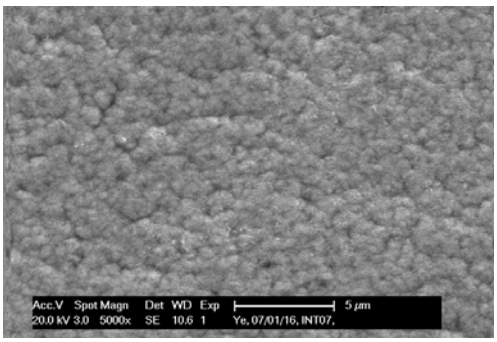

Fig. 6 SEM image showing surface feature of Fe-W (31 at. % of W)

thermodynamic point of view. In general, the hardness of Fe-W alloys is slightly higher than that of Co-W alloys. A slight increase in hardness is noticed with indentation depth because it monotonically starts sensing the hardness of the substrate material. Neither on Fe-W nor on Co-W coatings, radial-median cracks were not noticed inside the indentation volume even at high indentation loads.

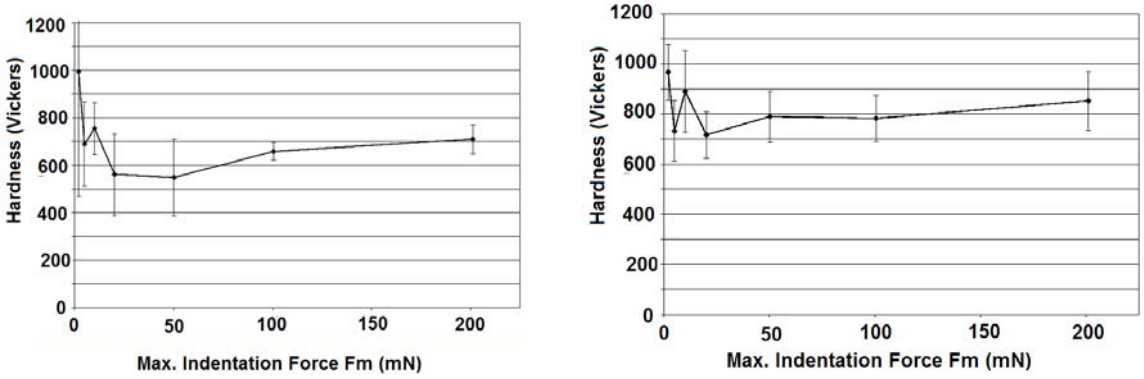

a b

Fig. 7 Vickers hardness derived from nanoindentation tests done at different indentation forces for (a) electrodeposited Co-W, and (b) Fe-W

3.2. Cracking of electrodeposited Co-W and Fe-W coatings

In this study, the position of an advancing crack in indentation was determined. Small changes in the direction of local stress fields were recorded at specific times and the position of corresponding changes in the direction of the crack was determined after the completion of the growth sequence. The crack face was then examined either optically or by scanning electron microscopy. The definition of failure can be the onset of cracking around the indenter or spalling of the coating. The crack front appears as a series of concentric rings (Fig. 8, b). Circumferential cracks were not noticed around indentations made at maximum load of 50 mN (Fig. 8, a).

The hardness of substrate material plays an important role in the wear behavior of coatings. The load applied onto the coating must be taken up by both the coating and substrate. The deformation of coatings and substrate, and contact stress distribution at the interface between the coating and substrate, depend strongly upon hardness of the substrate. The failure modes of electrodeposited Co-W coatings induced during Rockwell C test. Fig. 9, a shows delamination around the indentation area, whereas a large spalling is observed on the other coatings tested at a load above 2 kN (Fig. 9, b), at the side and forward rims of the indents. The cutting action inside the indentation, removed the grids and formed chips near the forward rim of the indent. This indicates the adhesion of the Co-W coatings is slightly better on copper substrates than on steel ones.

In earlier studies of hard Co-W and Fe-W electrodeposited films [16], the physical-mechanical properties of substrates have been almost ignored.

The indentation with a Vickers pyramid indenter (Fig. 10) is quite drastic test on brittle coatings due to the sharp contact [13]. On electrolytic Fe-W coatings deposited on copper, radial cracks are noticed in the indented area (Fig. 10, a). These radial cracks appear more and more frequently towards the rim of the indentation area (Fig. 10, c), at which point flexure is the largest. The induced tensile stresses are at maximum at the rim and radial – median cracks appear there due to the complexity of loading with may result in more than one deformation mode.

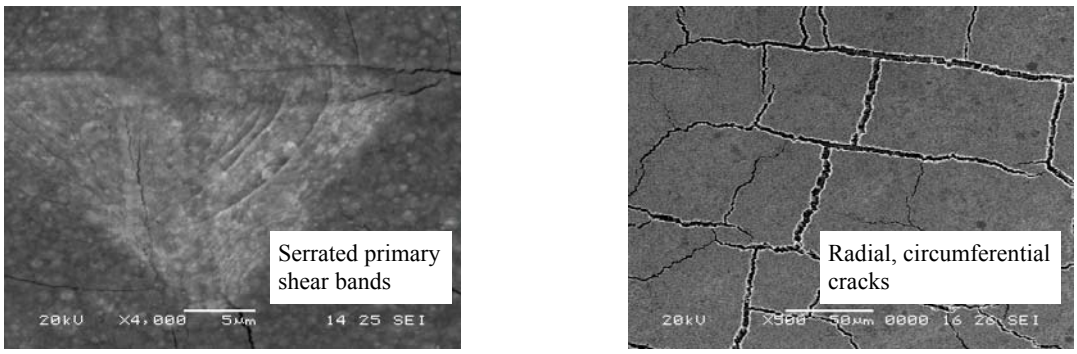

a b

Fig. 8 SEM illustrated crack formation induced by Vickers indenter on CoW (25 at. % of W) electrodeposited on polished Cu substrate (a), and ball indenter on FeW (28 at. % of W) electrodeposited on polished Cu substrate (b)

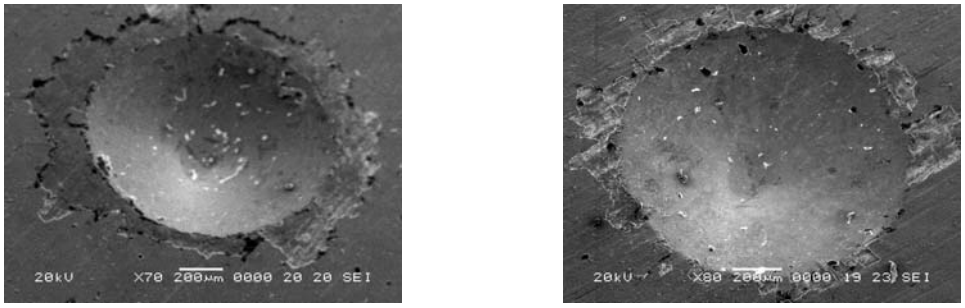

a b

Fig. 9 SEM pictures of Rockwell C indents on electrodeposited Co-W CoW (25 at. % of W) coats deposited on tempered steel (a) and copper (b)

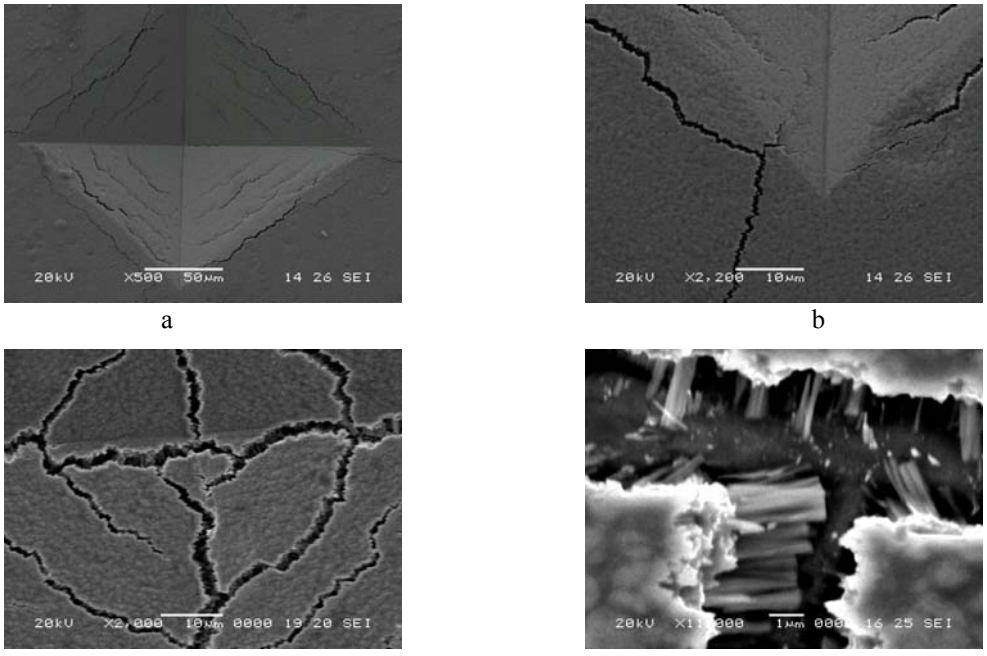

a b c d

Fig. 10 Coating failure modes on Fe-W (28 at. % of W) coating under Vickers indenter: top view (a), radial crack close to rim of indenter (b), vicinity of indentation area (c), cross-section of cracked zone on coating (d)

The trough-thickness cracks are likely located at the elastic-plastic boundary in substrates. The coating covering plastic region should deform, mostly likely elastically, to accommodate the Vickers indentation. We assume that the film beyond the plastic zone is damped during indentation. It should be noted that the formation of such radial and/or circumferential cracks is common to hard and brittle coatings [14, 21].

It was demonstrated experimentally [15] for thin hard coatings on soft substrates that critical tensile stresses for crack formation are not only outside the indentation volume, but also inside the imprint. Indentation test can be used to assess the flow stress behaviour over the strain range 2-16 or 18 % [13]. This statement applies fully to indentation test with various indenters, especially for materials like iron and steel, for coatings flow stress exhibited or decreasing trend with increasing strain [3].

4. Conclusions

1. Ammonia-citrate baths possessing the required buffer capacity for the electrodeposition of nanocrystalline and smooth Co-W and Fe-W alloys are proposed.

2. A qualitative study of the mechanical behavior of electrodeposited Co-W and Fe-W alloys was done by different indentation methods. The indentation parameters affect the behavior of the coating-substrate system especially when both deform plastically. It was shown that in order to suppress noncohesive failure and to ensure only adhesive failure of the coating, it is necessary to use an indenter with a large indentation angle. It was demonstrated that for electrodeposited thin hard coatings of Co-W and Fe-W on soft substrates, the critical tensile stresses for crack formation are outside the indentation volume.

3. Some limitations in the current analysis should be confirmed. We have considered only a monotonic loading to analyze crack evolution from initiation to failure. At no point in our experiments, the indenter was unloaded and reloaded since literature mentions that cracks can expand in size on unloading. Thus the median failure mode can be highly deleterious in brittle layer systems. In this case median-radial crack interaction is pronounced, highlighting the complexity of failure when more than one mode is present.

Acknowledgement

Financial support for this study was provided by EU INTAS program, Brussels, Belgium (INTAS Ref. Nr.05-104-7540).

References

1. **Miller, R.A.** Curent status of thermal barrier coatings – an overview. -Surf. Coat. Technol., 1987, 30, p.1-11.
2. **Podgornik, B.** Coated machine elements – fiction or reality? -Surf. Coat. Technol., 2001, 146-147, p.318-323.
3. **Gupta, B.K, Bhushan, B.** Mechanical and tribological characterization of hard carbon coatings for magnetic recording heads. -Wear, 1995, v.190 (1), p.110-122.
4. **Datta, M., Landolt, D.** Fundamental aspects and applications of electrochemical microfabrication. -Electrochim. Acta, 2000, v.45, No.15-16, p.2535-2558.
5. **Donten, M., Stojek, Z., Osteryoung, J.G.** Voltammetric, optical, and spectroscopic examination of anodically forced passivation of Co-W amorphous alloys. - J. Electrochem Soc., 1993, 140, p.3417.
6. **Habazaki, H., Kawashima, A., Asami, K., Hashimoto, K.** The effect of tungsten on the corrosion behavior of amorphous Fe-Cr-W-P-C alloys in 1M HCl. - J. Electrochem. Soc., 1991, 138, p.76.
7. **Donten, M., Cesiulis, H., Stojek, Z.** Electrodeposition and properties of Ni-W, Fe-W and Ni-Fe-W amorphous alloys. A comparative study. -Electrochimica Acta, 2000, v.45, N.20, p.3389-3396.
8. **Donten, M., Stojek, Z., Cesiulis, H.** Formation of nanofibres in thin layers of amorphous W alloys with Ni, Co and Fe obtained by electrodeposition. -J. Electrochem. Soc., 2003, v.150(2), p.C95-C98.
9. **Cesiulis, H., Baltutiene, A., Donten, M., Donten, M.L., Stojek, Z.** Increase in rate of electrodeposition and in Ni(II) concentration in the bath as a way to control grain size of amorphous / nanocrystalline Ni-W alloys. -J. Solid State Electrochem., 2002, v.6, No.4, p.237-244.
10. **Grabco, D.Z., Dikusar, A.I., Petrenko, V.I, Harea, E.E, Shikimaka, O.A.** Micromechanical proprieties of Co-W alloys electrodeposited under pulse conditions. -Elektronnaya Obrabotka Materialov (Surface Engineering and Applied Electrochemistry), 2007, 1, p.16-24.
11. **Younes, O., Zhu, L., Rosenberg, Y., Shacham-Diamand, Y., Gileadi, E.** Electroplating of amorphous thin films of tungsten/nickel alloys. -Langmuir, 2001, v.17, No.26, p.8270-5.
12. **Belevsky, S., Dikusar, A., Tsyntsaru, N., Celis, J.P.** Sliding and wear-resistance of electrodeposited cobalt-tungsten coatings: Dependence of synthesis parameters. -Proc. Int. Conf. Baltrib, 2007, p.111-116.
13. **Korsunsky, A.M., Gurk, M.R., Bull, S.J., Page, T.F.** On the hardness of coated systems. -Surf. Coat. Technol., 1998, p.171-183.
14. **Lawn, B.R., Wilshaw, T.R.** Indentation fracture: principles and applications. -J. Mater. Sci., 1975, v.10(6), p.1049-1081.
15. **Pelletier, H., Krier, J., Mille, P.** Characterization of mechanical properties of thin films using nanoindentation test. -Mechanics of Materials, 2006, 38(12), p.1182-1198.
16. **Nix, W.D.** Mechanical properties of thin films. -Metall. Trans. A, 1989, v.20A, p.2217-2245.
17. **Cesiulis, H., Podlaha-Murphy, E.J.** Electrolyte considerations of electrodeposited Ni-W alloys for microdevice fabrication. -Materials Science (Medziagotyra), 2003, v.9, No4, p.324-327.
18. **Cesiulis, H., Donten, M., Donten, M.L., Stojek, Z.** Electrodeposition of Ni-W, Ni-Mo and Ni-Mo-W alloys from pyrophosphate baths. -Materials Science (Medziagotyra), 2001, 7(4), p.237-241.
19. **Zakharov, E.N., Gamburg, Y.D.** Electrochemical production and properties of cobalt alloys with phosphorous and tungsten. -Protection of Metals, 1999, v.35(4), p.335-337.
20. **Kotry, S., Šucha, L.** Handbook of Chemical Equilibria in Analytical Chemistry. -New York: Ellis Horwood Ltd., 1985.
21. **Vasauskas, V.** Brittleness and fracture of materials in indentation. -Mechanika. -Kaunas: Technologija, 2003, No.6(44), p.5-12.

V. Vasauskas, J. Padgurskas, R. Rukuiža, H. Cesiulis, J.-P. Celis, D. Milčius, I. Prosyčevas

ELEKTROLITINIŲ NANOKRISTALINIŲ VOLFRAMO-KOBALTO IR VOLFRAMO-GELEŽIES DANGŲ PLYŠIŲ SUSIDARYMO BŪVIS

R e z i u m ė

Mechaninės inžinerijos srityje, siekiant sumažinti trintį ir dilimą, pastaruoju metu didėja susidomėjimas mikrometrinio storio dangomis. Šiame darbe yra nagrinėjamas elektrolitiniu būdu gautų Co-W ir Fe-W dangų deformavimas, panaudojant įspaudimo bandymus ir nustatant tokių elektrolitinių sluoksnių paviršių mikroskopines savybes. Be to, šis tyrimas grindžiamas plastinės deformacijos laukų įspaudimo bandyme analize, ypač gūbrelio susidarymo aplink įspaudą mechanizmo susidarymui.

V. Vasauskas, J. Padgurskas, R. Rukuiža, H. Cesiulis, J.-P. Celis, D. Milčius, I. Prosyčevas

CRACKING BEHAVIOR OF ELECTRODEPOSITED NANOCRYSTALLINE TUNGSTEN-COBALT AND TUNGSTEN-IRON COATINGS

S u m m a r y

The use of micrometer thick coatings in tribosystems now is of increasing interest in the area of mechanical engineering to reduce friction and wear. This work was initiated to analyse critically the deformation of electrodeposited Co-W and Fe-W coatings resulting from indentation tests, and to identify the microscopic features of the surfaces of such electrodeposited layers. On other hand, the present work focuses on an improved understanding of the plastic deformation field of the indentation made in thin layer deposited on a substrate, especially the mechanisms formation of the pile-ups around the indenter.

В. Васаускас, Ю. Падгурскас, Р. Рукуйжа, Г. Цесюлис, Ж.-П. Целис, Д. Мильчюс, И. Просычев

ИССЛЕДОВАНИЕ ОБРАЗОВАНИЯ ТРЕЩИН ЭЛЕКТРОЛИТИЧЕСКИХ НАНОКРИСТАЛИЧЕСКИХ ВОЛЬФРАМО-КОБАЛЬТОВЫХ И ВОЛЬФРАМО-ЖЕЛЕЗНЫХ ПОКРЫТИЙ

Р е з ю м е

В инженерной механике для уменьшения трения и износа в настоящее время возрастает интерес к использованию в трибосистемах покрытий микрометрической толщины. В настоящем исследовании испытаниями вдавливанием анализируются полученные Co-W и Fe-W электролитическим путем покрытия и определяются микроскопические свойства таких поверхностных слоев. С другой стороны исследование базируется на анализе полей пластической деформации, полученной при вдавливании на покрытие, сформированном на подложке, особенно на механизмее образования наплыва вокруг отпечатка.

Received May 08, 2008